ACS APPLIED MATERIALS & INTERFACES

Research Article

www.acsami.org

Evaluation of the Spectral Response of Functionalized Silk Inverse Opals as Colorimetric Immunosensors

Kelly A. Burke,[†,§,∥,⊥] Mark A. Brenckle,[†,⊥] David L. Kaplan,[*,†] and Fiorenzo G. Omenetto[*,†,‡]

[†]Department of Biomedical Engineering, and [‡]Department of Physics, Tufts University, 4 Colby Street, Medford Massachusetts 02155, United States

[§]Department of Chemical and Biomolecular Engineering, and [∥]Polymer Program, University of Connecticut, Storrs, Connecticut 06269, United States

Supporting Information

ABSTRACT: Regenerated silk fibroin is a high molecular weight protein obtained by purifying the cocoons of the domesticated silkworm, *Bombyx mori*. This report exploits the aqueous processing and tunable β sheet secondary structure of regenerated silk to produce nanostructures (i.e., inverse opals) that can be used as colorimetric immunosensors. Such sensors would enable direct detection of antigens by changes in reflectance spectra induced by binding events within the nanostructure. Silk inverse opals were prepared by solution casting and annealing in a humidified atmosphere to render the silk insoluble. Next, antigen sensing capabilities were imparted to silk through a three step synthesis: coupling of avidin to silk surfaces, coupling of biotin to antibodies, and lastly antibody attachment to silk through avidin−biotin interactions. Varying the antibody enables detection of different antigens, as demonstrated using different protein antigens: antibodies, red fluorescent protein, and the beta subunit of cholera toxin. Antigen binding to sensors induces a red shift in the opal reflectance spectra, while sensors not exposed to antigen showed either no shift or a slight blue shift. This work constitutes a first step for the design of biopolymer-based optical systems that could directly detect antigens using commercially available reagents and environmentally friendly chemistries.

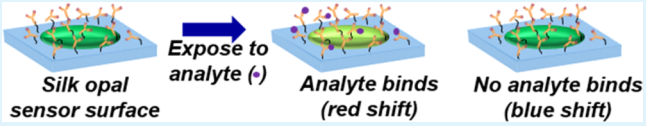

KEYWORDS: *silk fibroin, immunosensor, inverse opal, biopolymer, antibody, antigen, biosensor, photonic crystals*

1. INTRODUCTION

The field of biosensors[1−3] has been of increasing interest in recent years due to the need for inexpensive, highly selective devices for measurement of physiologically relevant analytes in biofluids. These devices consist of two main parts: a capturing component to select for the analyte of interest and a signal transduction component to convert the selection event into a measurable form. In this context, biosensors are unique in that they employ a diverse subset of biological agents, such as antibodies, cells, or nucleic acids, to capture the analyte of interest. Antibodies[4] are particularly well-suited for this purpose because they are highly specific for analytes, are highly conserved in their chemical structure, can be prepared against a wide-variety of antigens, and can be scaled up and prepared in vitro using hybridoma technology.[5,6] The conserved structure allows antibody-based sensor designs to function as interchangeable families of sensors, thereby improving their versatility.

Signal transduction components also vary, but for antibody-based biosensors, signal transduction is commonly accomplished by measuring optical density (OD), fluorescence signals, electromagnetic resonance, or electrical impedance (for recent reviews in affinity-based biosensors, the reader is directed to refs 7−9). In fluorescence-based and optical density sensors, the analyte is detected indirectly using a fluorophore or enzyme-conjugated secondary antibody, respectively, that also binds to the analyte of interest. Indirect detection methods are widely used in the laboratory (e.g., in enzyme-linked immunosorbent assays, ELISAs) because they are readily adapted to various analytes; however, nonspecific binding of secondary antibodies can lead to high background signals and reduce the sensitivity of the assay. Direct binding of the analyte may be detected without the use of a secondary antibody in resonance and impedance-based sensors (e.g., using quartz crystal microbalance (QCM)[10−12] or surface plasmon resonance (SPR),[13−16] where changes in frequency are observed in the sensor when binding occurs. Direct measurement of analytes by affinity biosensors[17] is desirable, but these signal transduction mechanisms can be more difficult and expensive to scale up than indirect methods due to the expensive equipment required and the labile nature of the chemistries involved. An antibody-based platform that enables direct optical measurement of analyte binding using lower cost and portable components can therefore enhance sensing by offering the versatility of antibody sensing, the ability to scale up and customize sensors, and the advantage of direct observation of analytes. In this work, the development of such a biodegradable sensor is investigated.

Silk fibroin produced by *Bombyx mori* is a segmented protein consisting of alternating hydrophilic and hydrophobic domains

Received: February 22, 2016
Accepted: May 24, 2016

DOI: 10.1021/acsami.6b02215
ACS Appl. Mater. Interfaces XXXX, XXX, XXX−XXX

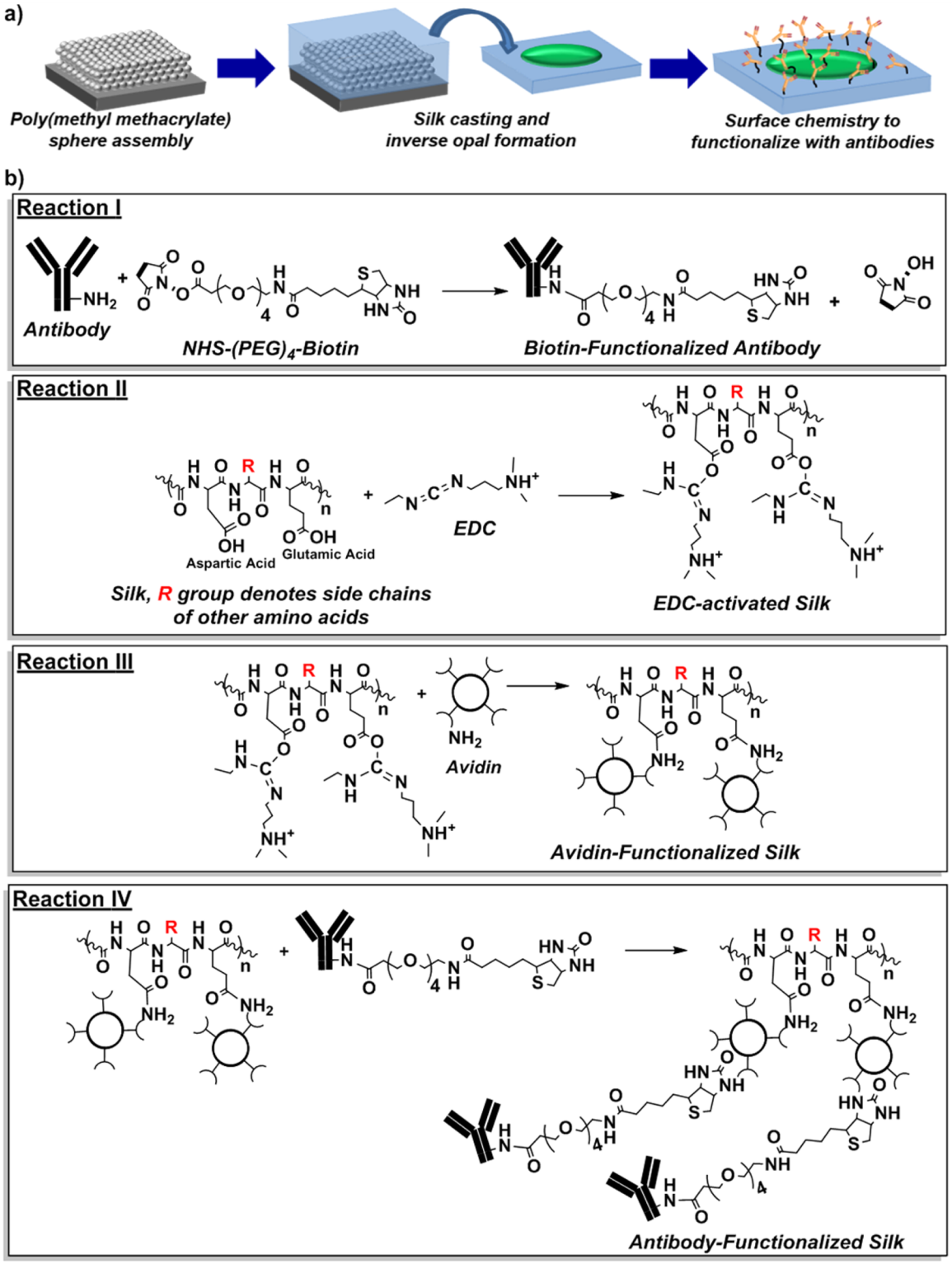

Figure 1. Sensor system schemes and generalized approach. (a) Fabrication scheme for sensing system investigated. Sensors were fabricated by first nanopatterning silk films to introduce colorimetric optical response. Crystallization of the film allows for chemistry to be carried out on the surface, followed by conjugation of antibodies to modulate response. (b) Reaction schemes for attachment of antibody to silk. Reaction I, biotinylation of antibody; Reaction II, EDC activation of silk; Reaction III, avidin coupling to activated silk; Reaction IV, conjugation of avidin modified silk to biotinylated antibodies.

of varying lengths.[18,19] The hydrophilic blocks consist of proportions of tyrosine (Y), glutamic acid (E), and aspartic acid (D), which contain or are easily modified with carboxylic acid functional groups as excellent target sites for the coupling of antibodies; roughly 6.6 mol % of the protein.[20,21] The hydrophobic domains contain repeats of glycine (G), alanine (A), and serine (S) amino acids in the sequence GAGAGS, and hydrogen bonding between hydrophobic segments results in a

DOI: 10.1021/acsami.6b02215
ACS Appl. Mater. Interfaces XXXX, XXX, XXX−XXX

β sheet (physical cross-links) secondary structure that can be tuned by processing methods[22−25] to control the mechanical properties, stability, and degradation rate of the material. Silk materials are unique in comparison to other proteins as they are mechanically robust and can withstand a variety of processing techniques involving aqueous and organic solvents, as well as thermal treatments to at least 160 °C in a dry atmosphere and 121 °C in a humidified atmosphere.[25−28] A variety of processing conditions have been leveraged to generate a variety of optical devices based on silk, including inverse opals,[29−32] photonic crystals,[33−35] holograms,[36] and other environmentally sensitive structures.[37−41] Further, the biocompatibility and degradability of silk has been used to build technical devices well-suited to the biotic/abiotic interface.[42]

Previously, silk periodic lattices[34] have been shown to display a colorimetric shift in response to nonspecific binding of glucose solutions. The present work seeks to explore the potential for analyte specificity of this class of nanostructured geometries. Here, aqueous chemistries and commercially available reagents are used to functionalize nanostructured silk surfaces with antibodies. The antibodies function as capture elements for the molecule of interest, and the antibody's highly conserved structure enables a versatile material that may be tailored for different analytes. The resulting system, an optical platform for the direct sensing of analytes, combines the use of protein solubility, aqueous surface chemistries, and a templated nanostructure. While this work focuses on silk inverse opal nanostructures as the transduction element, other silk optical structures (e.g., periodic lattices) may also be investigated in the future. The work described below provides an evaluation of a possible strategy to engineer sensors based on functionalized nanostructured silk and is anticipated to be applicable to other silk structures as a versatile analyte detection platform.

2. EXPERIMENTAL SECTION

2.1. Reagents. Silk cocoons were purchased from Tajima Shoji Company (Japan). Sodium carbonate, lithium bromide, 3,3′,5,5′-tetramethylbenzidine (TMB) liquid substrate system, and 1,1,1,3,3,3-hexafluoroisopropanol (HFIP) were purchased from Aldrich Chemical Co. (St. Louis, MO). Phosphate buffered saline (1× PBS), methanol (certified ACS grade), 2-propanol (laboratory grade), acetone (Optima grade), sulfuric acid (H_2SO_4) (certified ACS grade), Pierce NeutrAvidin, 1-ethyl-3-(3-(dimethylamino)propyl)carbodiimide hydrochloride (EDC), 2-(*N*-morpholino)ethanesulfonic acid (MES) buffer, Tween 20, Slide-a-Lyzer dialysis cassettes (3500 MWCO), Costar 3925 high binding black 96-well polystyrene plates with black bottom, Costar 3601 high binding black 96-well polystyrene plates with clear bottom, Zeba Spin desalting columns (7K MWCO), Melon Gel IgG spin purification kit for the removal of albumin from antibodies (Pierce cat# 45206), and NHS-PEG4-biotin (this molecule contains four poly(ethylene glycol) (PEG) repeat units as a 29 Å spacer between *N*-hydroxysuccinimide (NHS) and biotin) were purchased from ThermoFisher Scientific (Pittsburgh, PA). Biotinylated horseradish peroxidase was obtained as component B of VectaStain ABC kit (Vector Laboratories, Bulingame, CA). All antibodies were purchased from Abcam, Inc. (Cambridge, MA). Red fluorescent protein was purchased from Biovision (Milpitas, CA) and Alexafluor conjugated cholera toxin beta subunit was purchased from Life Technologies, Inc. (Grand Island, NY). Reverse osmosis water (18 mΩ, dH_2O) was obtained from an in-house purification system. 250 nm PMMA nanospheres were purchased from Phosphorex Inc. (Hopkinton, MA), and PMMA 950 C2 solution was obtained from Microchem Inc. (Newton, MA).

2.2. Instruments. Freeze-drying of frozen silk solutions was accomplished using a Labconco lyophilizer (Kansas City, MO) operating at 0.008 Torr and −83 °C. Absorbance and fluorescence measurements of samples in plates were acquired using a SpecraMax M2 plate reader controlled by SoftMax Pro software (v. 6.2.2) from Molecular Devices (Sunnyvale, CA). A portable spectrometer (USB 2000, Ocean Optics Inc., Dunedin, FL) was used for collection of reflectance spectra on the opals using the associated Spectra Suite software.

2.3. Purification of Silk Fibroin. Cocoons of *Bombyx mori* were processed by degumming for 30 min in a boiling 0.2 M sodium carbonate solution, rinsing and drying degummed fibers, dissolving in a 9.3 M lithium bromide solution, and dialysis for 3 days in a 3500 molecular weight cutoff (MWCO) dialysis cassette against distilled water to give an aqueous silk solution, as described previously.[43] The resulting 5−6 wt % silk fibroin solution was frozen using a dry ice slurry (CO_2/2-propanol) and lyophilized for 4 days to yield dry silk fibroin protein.

2.4. Preparation of Silk Fibroin Films. Dry silk fibroin protein was dissolved in HFIP (2 wt %) and cast into the wells of a 96 well high protein binding plate (30 μL/well). The plates were wrapped in aluminum foil and placed in a fume hood for 4 days, over which an increase in viscosity was observed as the HFIP evaporated. The plates were uncovered after 4 days to allow residual HFIP to evaporate, yielding a transparent film adhered to the bottom of the well. The silk was then treated for 10 min with a methanol solution (by volume 90% methanol and 10% distilled water (dH_2O)) to induce β sheet formation in the silk film. The films were then washed five times with dH_2O to remove any soluble protein, leaving transparent and water-insoluble films. Once hydrated, silk films were stored hydrated at 4 °C for up to a week. Note, throughout all of these steps, care was taken to ensure that the pipet tip did not touch the well to prevent damage to the silk film.

2.5. Preparation of Silk Fibroin Inverse Opals. Silk fibroin inverse opals were fabricated based on previously investigated procedures.[28,31] Briefly, a 100 nm thick layer of poly(methyl methacrylate) (PMMA) (PMMA 950 C2, Microchem Inc., Newton, MA) was deposited on a clean silicon wafer by spin coating. A single droplet of a suspension of 250 nm diameter PMMA nanospheres (Phosphorex Inc., Hopkinton, MA) was then pipetted onto the surface. Drying at 95 °C on a hot plate induced self-assembly of the spheres, leading to a 3.5 mm diameter opal. A 7.5% aqueous silk fibroin solution (100 μL) was then cast on top of each opal in a roughly 6 mm diameter area and allowed to dry under ambient conditions. The resulting films were water-vapor annealed under reduced pressure at 95 °C for 24 h to induce β-sheet crystallization, and then immersed in acetone for 24 h to dissolve the PMMA nanospheres and release the films from the silicon substrates, producing silk inverse opal films. An image showing a typical inverse opal structure from this process can be found in the Supporting Information.

2.6. Attachment of Biotin to Antibody. Antibodies were attached to silk films or opals using a four step route (Figure 1b). The studies reported herein used antibodies that were purchased both with and without biotin functionalization. For unconjugated antibodies, an additional synthetic step was performed to attach biotin to the antibody (Figure 1b, Reaction I). The biotinylation of an anti-goat IgG is described here as an example. Because this antibody contained albumin, the antibody (84 μg antibody/purification) was first purified using the Pierce Melon IgG kit according to manufacturer's instructions. The purified antibody was then diluted to a concentration of 168 μg/μL and loaded onto a HisPur Ni-NTA Spin column (Pierce). The antibody was allowed to bind for 10 min at 20 °C with gentle rocking before centrifuging (700*g* for 2 min). The flow through was discarded and the column was washed with 1× PBS before centrifuging and discarding flow through for a total of four washes. NHS-PEG4-biotin (2 mg) was then dissolved in 1× PBS (200 μL). The NHS-PEG4-biotin solution was diluted with 1× PBS (10 μL of the NHS-PEG4-Biotin solution, 190 μL of 1× PBS) and was added to the plugged column. After a 30 min incubation at 20 °C, the tube's stopper was removed, and the tube's contents were washed four times with 1× PBS using the centrifuge to elute the wash, which was discarded as waste. Finally, the purified antibody was released from the

DOI: 10.1021/acsami.6b02215
ACS Appl. Mater. Interfaces XXXX, XXX, XXX−XXX

column by incubating the stoppered column with an imidazole solution (400 μL, 0.2 M) for 10 min at 20 °C before eluting by centrifugation (2 min at 700*g*).

2.7. Conjugation of Avidin to Silk. To attach avidin to silk (Figure 1b, Reactions II–III), water was removed from the wells of the plate using a micropipettor and aqueous EDC solution (100 μL of 2 mM in MES buffer, pH 6.0) was added to the well containing the film. For covalent coupling of avidin, activation of the carboxylic acid groups on the silk proceeded for 15 min at 20 °C before removal of the EDC solution by micropipettor and addition of an aqueous avidin solution (100 μL/well, 2.5 mg/mL avidin in 1× PBS, pH 7.4). The conjugation reaction was allowed to proceed for 4 h at 20 °C before removal of the solution, washing of the wells with 1× PBS containing 0.5% Tween 20 (200 μL/wash, repeated 5 times), and finally washing with dH_2O to remove PBS and Tween from the wells (200 μL/wash, repeated 5 times) to yield the avidin-functionalized silk.

2.8. Attachment of Antibody to Silk. To attach biotinylated antibodies to the avidin-functionalized silk (Figure 1b, Reaction IV), the silk surface was first treated with a blocking solution (2.5% nonfat dry milk with 1% Tween 20) for 1 h at 20 °C to prevent nonspecific binding of the antibody. The antibodies were then diluted in 1× PBS (pH 7.4) to a concentration of 750 μg/mL. Antibody solution (70 μL) was added to each well, and the conjugation was allowed to proceed for at least 4 h at 20 °C or overnight at 4 °C. After incubation, unbound antibody was removed by washing in the same manner as was described for the avidin step (5 washes with 1× PBS with 0.5% Tween 20 followed with 5 washes with dH_2O) to yield antibody-functionalized silk fibroin.

2.9. Assay for Avidin Attachment. Conjugation of avidin to silk was assayed using horseradish peroxidase (HRP) and TMB substrate. Biotinylated horseradish peroxidase was obtained as component B of VectaStain ABC Kit and was diluted to a working solution (100 μL component B in 10 mL PBS). Working solution (100 μL) was added to each well and incubated for 2 h at 20 °C before washing with PBS containing Tween 20 and water, as described previously for avidin attachment. TMB substrate was diluted to a working solution (1 mL TMB in 3 mL PBS), which was added to the wells (100 μL/well) and the reaction was allowed to proceed for 4 min before stopping the reaction with the addition of H_2SO_4 (50 μL, 2 N H_2SO_4). The oxidation of TMB, and thus the presence of biotinylated HRP and avidin, was quantified by measuring absorbance at 450 nm using the SpectraMax plate reader. Control wells without avidin were assayed in this manner at the same time for statistical analysis.

2.10. Assay for Antibody Attachment. Antibody attachment was measured using secondary antibodies conjugated with HRP. Polyclonal IgG antibodies were selected to be reactive for the species of the primary (silk-conjugated) antibody. To reduce nonspecific binding of the secondary antibody, the wells were blocked (2.5% NFDM and 1% Tween 20 in 1× PBS) for 1 h at 20 °C. The wells were then exposed to the secondary antibody (10 ng/μL in 1× PBS; ∼ 0.6 pmol/μL) for 2 h, and washed as described above. The wells were then exposed to TMB, the reaction quenched with H_2SO_4, and absorbance was measured with the plate reader, as described above for the avidin attachment assay. Control wells with avidin but without antibody were also assayed at the same time for statistical analysis.

2.11. Fluorescence Assays for Antigen Binding. Binding of red fluorescent protein was assessed by incubating silk sensors (with anti-RFP conjugation) and controls (without anti-RFP conjugation) prepared on 96 well black bottom plate with an aqueous RFP solution (412 ng/μL RFP in 1× PBS; ∼15 pmol/μL). Alternatively, AlexaFluor conjugated cholera toxin beta subunit was incubated in wells (125 ng/μL in 1× PBS; ∼11 pmol/μL) with and without cholera toxin antibodies. The antigen was incubated for 2 h at 20 °C, washed as described above before fluorescence was measured using the plate reader.

2.12. Analysis of Antigen Binding by Spectral Shift. Silk inverse opal films were mounted to the underside of 48 well filter-bottom microwell plates (Millipore Inc., Darmstadt, Germany) that had the filter removed, with the aid of optical plate sealer as an adhesive. Antibody binding chemistry was then carried out on the films as described above. Control films containing avidin without the capture antibody were prepared by exposing the film to all of the same solutions except for the antibody binding solution, which differed in that it contained only the PBS buffer for the control samples. The reflectance spectra of the completed sensors were then measured across the visible spectrum (400–800 nm) using the portable spectrometer (USB 2000, Ocean Optics Inc., Dunedin, FL), and the samples were exposed to either a red fluorescent protein solution in 1× PBS (412 ng/μL) or a buffer only solution for 2 h to allow for binding. The samples were then washed thoroughly with 1× PBS containing 0.5% Tween 20 and subsequently water, as described above, to remove unbound protein. The reflectance spectra were then measured a second time. Spectra were baseline corrected and fit to a single Gaussian peak to determine the peak wavelength and amplitude. Data from spectra collected before and after antigen exposure and washing steps were compared to detect antigen binding.

2.13. Statistical Methods. Data are expressed as mean ± standard deviation (SD). Statistically significant differences were determined by one-way analysis of variance (ANOVA) and the Tukey post-test. Statistical significance was accepted at $p < 0.05$ and indicated in the figures as described.

3. RESULTS AND DISCUSSION

The biosensing system (Figure 1a) consists of a patterned silk substrate conjugated with antibodies. As a generalized fabrication approach, the silk is cast into a nanopatterned inverse opal[28] and β-sheet crystallization is carried out to render the silk insoluble in water before conjugating antibodies to the surface. This scheme holds advantages over other methods because it ensures that the antibody active sites will be accessible at the surface of the film and not buried in the bulk of the substrate. Additionally, this scheme prevents the possibility of conjugated biomolecules interfering with β sheet crystallization, which is necessary for water stability of the system. However, the β-sheet crystals produced by the large hydrophobic domains in the protein renders many of the side chains unavailable for conjugation. Conjugation of antibodies was thus carried out on the carboxylic acid side chains of the glutamic acid and aspartic acid residues in the hydrophilic domains using avidin–biotin interactions.[44,45] This approach was selected due to the strength, specificity, and stability of this noncovalent interaction, and its ease of integration with different sensing components, including antibodies. This approach was applied to the glutamic acid and aspartic acid residues in three steps (Figure 1b): conjugation of biotin to the antibody (Reaction I), conjugation of avidin to silk (Reactions II–III), and finally conjugation of the antibody to silk (Reaction IV). This approach was a robust and repeatable method for the conjugation of antibodies to silk.

The conjugation of avidin to silk was confirmed by assay with biotinylated horseradish peroxidase (HRP), which binds to avidin and oxidizes tetramethylbenzidine (TMB) in the presence of hydrogen peroxide to form a colorimetrically detectable product. Figure 2a shows that silk-avidin has a roughly 7-fold higher absorbance of 3,3′,5,5′-tetramethylbenzidine diimine at 450 nm than silk without avidin, indicating that more biotinylated HRP attached to the silk-avidin substrates than the silk substrates ($p < 0.001$, n = 6) and the successful conjugation of avidin to silk. Figure 2a also compares noncovalent and covalent attachment of avidin to the silk surface. Covalent attachment was achieved by activating the carboxylic acid groups on the silk surfaces using EDC (as described in the Experimental Section) before depositing avidin, while noncovalent attachment added the avidin to the silk surface without the EDC step. Figure 2a shows that there

DOI: 10.1021/acsami.6b02215
ACS Appl. Mater. Interfaces XXXX, XXX, XXX–XXX

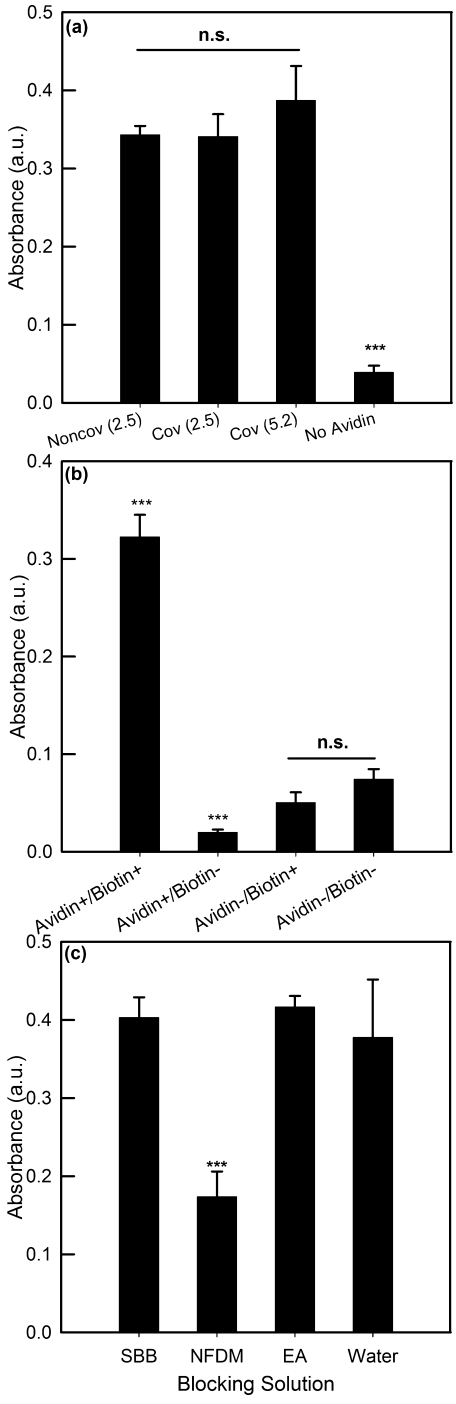

Figure 2. Assessment of antibody conjugation reactions onto silk substrates. (a) Attachment of avidin to silk, as assayed by HRP and TMB. Avidin was noncovalently deposited at 2.5 mg/mL (Noncov (2.5)) and covalently attached either at 2.5 mg/mL (Cov (2.5)) or 5.2 mg/mL (Cov (5.2)). Control surfaces are silk only (no avidin). (b) Binding of antibodies to silk and avidin-functionalized silk, as assayed with a horseradish peroxidase-conjugated secondary antibody and TMB (significance noted relative to biotinylated antibody attaching to silk surface without avidin (avidin-/biotin+). (c) Blocking of nonspecific antibody attachment to avidin-functionalized silk surfaces using 1% Tween 20 with Pierce SuperBlocking buffer (SBB), 2.5 wt/v % nonfat dry milk (NFDM), 10 v/v% ethanolamine, and water, as assayed by a horseradish peroxidase-conjugated secondary antibody and TMB (significance noted relative to wells blocked with water). p values for significance: ***$p < 0.001$.

was no statistically significant difference between covalent and noncovalent attachment, and this is thought to be due the small amount of glutamic acid and aspartic acid residues that are available in silk for conjugation, though this may be increased in the future through modification of serine residues.[46,47] Despite this, covalent attachment of avidin was continued because immobilization by covalent bonding was anticipated to enhance stability of avidin on the silk surface, though this would need to be confirmed with additional studies. Finally, increasing the avidin concentration from 2.5 to 5.2 mg/mL did not result in statistically larger amounts of avidin attached to silk, thus all subsequent experiments used a 2.5 mg/mL solution of avidin with the covalent coupling route to prepare the sensing surfaces.

The necessity both the avidin conjugation and the avidin−biotin interaction is shown in Figure 2b. Silk films before and after conjugation with avidin were exposed to primary antibodies with and without biotin functionalization. After removing unbound primary antibody (capture antibody) with IgG isotype, the samples were exposed to an HRP-conjugated anti-IgG antibody. Unbound secondary antibody was removed by a second washing step, and the substrates were again assayed by colorimetrically detecting 3,3′,5,5′-tetramethylbenzidine diimine, the oxidized product of TMB. The highest binding of antibody was for the silk-avidin surfaces exposed to biotinylated antibody (Figure 2b). These substrates have a significantly higher ($p < 0.001$) absorbance than silk-avidin substrates exposed to antibodies that were not conjugated with biotin, indicating that biotinylation was necessary to attach the antibody to the avidin-functionalized surface. Further, the silk-avidin surfaces exposed to the biotinylated antibody bound significantly more ($p < 0.001$) antibody than the silk surfaces without avidin functionalization. There is also a significant ($p < 0.001$) decrease in antibody binding to avidin-functionalized surfaces compared to surfaces without avidin, indicating that avidin may assist in reducing nonspecific antibody binding.

These results indicate that both avidin and biotin are necessary for the attachment of the antibody to the silk surfaces. In addition to demonstrating a successful route to antibody functionalization, these results also show that specific binding was more favorable than nonspecific binding. This is relevant given that hydrophobic regions of silk can bind many molecules nonspecifically.

To further reduce nonspecific binding of molecules to these surfaces, different blocking buffers were investigated (Figure 2c), which shows that 2.5% nonfat dry milk in water with 1% Tween 20 blocked significantly more nonspecific antibody attachment ($p < 0.001$) to silk-avidin surfaces than each of the following blocking solutions: 10 v/v% ethanolamine with 1% Tween 20, water with 1% Tween 20, and the commercially available Pierce SuperBlocking buffer with 1% Tween 20. Different linking spacers between the antibody and the biotin functional end were also investigated to determine if spacer length or hydrophobicity affected the amount of antibody conjugated to the silk-avidin surface, but no difference was found for the spacers studied (see the Supporting Information).

With successful conjugation of antibodies to the silk substrates, the versatility of the system was investigated. Here, the applicability of the conjugation scheme to different antibodies and the ability to detect antigens of different sizes without steric hindrance were investigated. Antibodies conjugated to silk films can be used to detect protein antigens of different sizes: antibodies (Figure 3a) (150 kDa), red

DOI: 10.1021/acsami.6b02215
ACS Appl. Mater. Interfaces XXXX, XXX, XXX−XXX

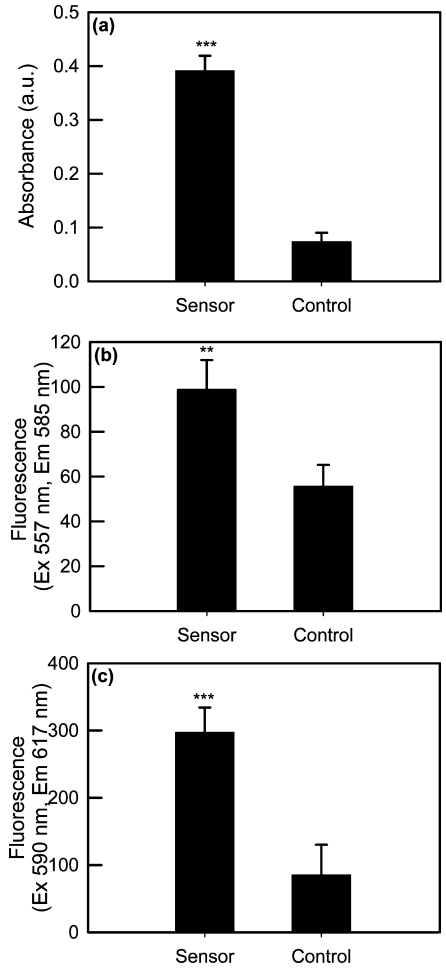

Figure 3. Binding of (a) antibodies, (b) red fluorescent protein, and (c) cholera toxin beta subunit to silk sensors is significantly higher (**$p < 0.01$ and ***$p < 0.001$) than that to control substrates that lack the capture antibody.

fluorescent protein (Figure 3b) (27.6 kDa), and cholera toxin beta subunit (Figure 3c) (11.4 kDa monomer, 57 kDa pentamer). These antigens were selected because they were protein targets that varied in molecular weight and because they were commercially available in a labeled (fluorophore or HRP enzyme) form, which enabled the use of a plate reader to assess binding prior to the reflectance-based studies. In all cases, the control sample (silk coupled with avidin but lacking capture antibodies) was treated identically to the antibody sample: blocked, exposed to antigen, washed, and optically analyzed in the same manner. Each of the sensors was found to have significantly more antigen bound than the control wells ($p < 0.001$ for Figure 3a, $p < 0.01$ for Figure 3b, and $p < 0.001$ for Figure 3c). This finding indicates that this system should be compatible with any commercially available antibody and that protein antigens are detectable over a wide range in sizes. These results also represent an improvement over previous attempts to conjugate antibodies to silk through similar means. Avidin/biotin based conjugation carried out in silk solution[48] and conformational-transition-assisted immobilization[49] suffered from a high degree of nonspecific binding of the functional proteins to the silk surface, leading to poor discrimination between the chemically modified samples and controls. As such, the previous methods could not be applied in a sensing system. The methods reported in this work illustrate a reduction in nonspecific binding, leading to antigen sensing by the modified films regardless of the antibody/antigen system tested.

The improved antibody conjugation scheme was then combined with a structured silk film optimized for optical transduction to complete the direct sensing system. Here, silk inverse opal structures were utilized to obtain a colorimetric shift in response to antigen binding events (Figure 4a). Silk inverse opals have reflectance spectra sensitive to the refractive index of the solution that permeates the structure, induced by a shift in the photonic band gap.[28] Bound antigens localized in the gaps of this structure cause a local increase in the effective index of refraction, leading to a red-shift in the reflectance spectra of the opals, in a manner analogous to the operation of a surface plasmon resonance (SPR) sensor. The high degree of surface area present in the nanoporous opal structure further improves the surface area for binding, and thus detection, within the system.

To detect antigens using reflectance spectra, silk opals conjugated with red fluorescent protein antibodies (hereafter "anti-RFP") were first prepared. Reflectance spectra were then acquired using a portable spectrometer before the antigen was exposed to the surface, as well as after antigen was exposed to the surface and the surface was washed to remove unbound antigen. Representative spectra for measurements taken before and after antigen exposure are shown in Figure 4b for sensing opals exposed to antigen (bottom), sensing opals not exposed to antigen (e.g., buffer vehicle only) (top), and control opals that lack antibody but were exposed to antigen (middle). A red shift in the peak of the reflectance spectra when the antigen bound to the sensing wells was observed, but overall there was a blue shift or no shift in the opals that either were not exposed to the antigen or did not include the capturing antibody. Small variations in the initial wavelength and intensity of the reflectance peak were also noted, which can be attributed to variations in measurement angle in the experimental setup. The sensors were therefore held fixed relative to the light source for the duration of the experiment to avoid the introduction of error in the measurement.

The average normalized shift in reflectance from independent experiments is reported in Figure 4c, where it is shown that the sensing opals exposed to antigens displayed a statistically significant ($p < 0.05$, $n = 4$) red shift compared to opals that either (1) contained capturing antibody but were not exposed to the antigen or (2) did not contain the capture antibody but were exposed to antigen. The red shift is understood in the context of SPR sensors, as briefly mentioned. The blue shift measured in the control samples is attributed to a decrease in the photonic crystal lattice pitch due to salt adsorption by the system from the saline buffers utilized in the chemical conjugation steps (see the Supporting Information). Based on the sensitivity of the inverse opal structure (430 nm/RIU), it was calculated that the minimum detectable concentration of analyte would be on the order of 50 ng/μL (see the Supporting Information), though this detection limit may decrease with system optimization.

The system described in this work represents a first step toward an immunosensing platform that leverages ambient processing techniques and portable, inexpensive measurement equipment, which may extend use to point of care locations that are difficult to access with other direct-transduction immunosensors. The mild aqueous processing conditions used for both the silk opal preparation and antibody conjugation schemes are compatible with the entrapment of bioactive

DOI: 10.1021/acsami.6b02215
ACS Appl. Mater. Interfaces XXXX, XXX, XXX−XXX

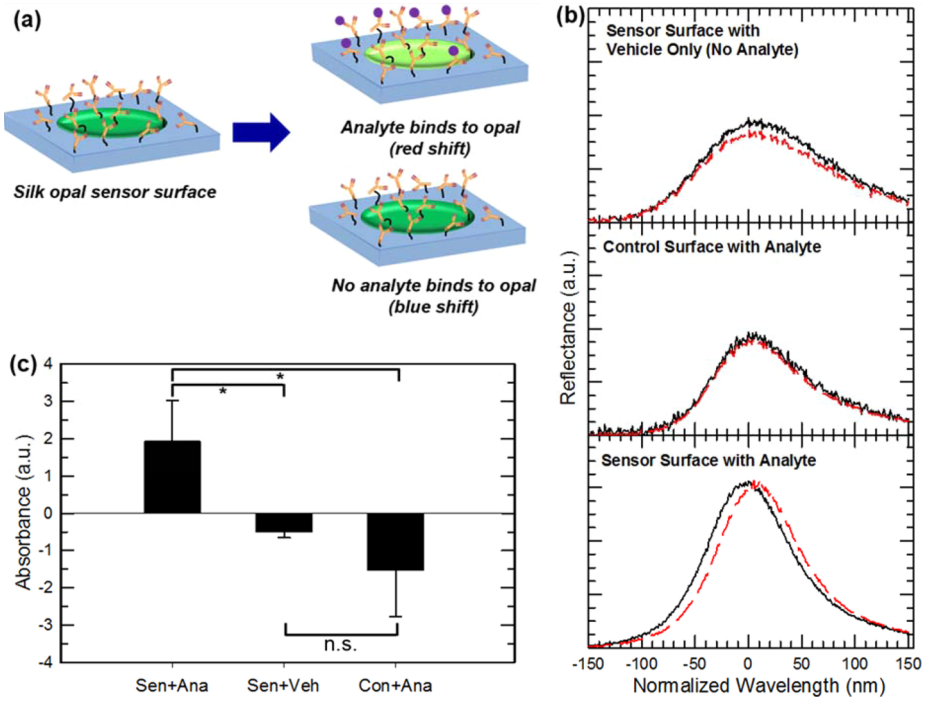

Figure 4. Colorimetric sensing of antibody−antigen binding. (a) Scheme of colorimetric sensing mechanism. Binding of antigen (RFP) within the silk opal matrix locally changes the effective refractive index of the permeating solution, leading to a color change. (b) Representative spectra of each tested sensor configuration before (solid black trace) and after (dashed red trace) exposure to analyte. Variation in intensity within each sample is due to difference in initial coupling angle with the light source and detector. (c) Normalized peak wavelength shift for sensor (abbreviated "Sen") and control (abbreviated "Con") surfaces probed with analyte (abbreviated "Ana") or buffer vehicle without analyte (abbreviated "Veh"). Asterisk (*) denotes statistical significance at $p < 0.05$; n.s. denotes no statistical significance.

molecules within the opals. To this end, horseradish peroxidase (HRP) was encapsulated within the silk opal, where it was found that the HRP encapsulation did not adversely affect opal formation and the HRP was still active within the opal (see the Supporting Information). The encapsulation of an enzyme may find use in more complex sensors, where the analyte detected does not need to be present in the fluid placed on the sensor, but instead may be a product of the enzyme acting on a molecule in that fluid. While it is recognized that not all bioactive molecules may remain functional after opal processing and that conditions may need to be optimized for different molecules, these findings highlight an additional advantage of the silk nanostructure sensing scheme and offer the potential for the development of two-stage sensing schemes that build upon the systems reported here.

This work demonstrated the direct detection of red fluorescent protein using a silk inverse opal nanostructure conjugated with capture antibodies. There were several key components that were critical to the generation of this functional material, including the aqueous processing of silk that permitted casting onto PMMA nanospheres, the formation of beta sheets that rendered the silk film's nanostructure insoluble, and the aqueous chemistries that lead to successful antibody functionalization while preserving opal nanostructure. A sensing inverse-opal constitutes a particularly compelling test device given its complex 3D nanostructure, in spite of the small reflectance change detected in the device response. Further tailoring and design of nanostructured films would offer the opportunity to enhance the spectral changes that are induced by antigen binding. In addition to investigating other nanostructures as transduction elements, future use of these materials as sensors for direct analyte detection will require detailed investigations of sensor performance,[50−53] including the effect of antigen concentration on spectral shift, overall sensitivity and selectivity for antigens, and performance in complex buffers. Further, the stability (e.g., thermal, pH) of the sensing surfaces will also need to be evaluated.

4. CONCLUSIONS

This work explored the use of a sensing platform that exploits the specificity of antigen−antibody interactions and the colorimetric transduction of nanostructured photonic crystal structures to sense the surrounding environment. Silk is a good candidate for this system because of its remarkable mechanical and thermal stability, ambient and versatile processing conditions, and assessable chemistries for functional group modification. The system as demonstrated allows for the conjugation of a family of IgG antibodies to nanostructured silk films, with the possibility for detection regardless of antigen size. Measurement of the colorimetric response was achieved with portable equipment, providing a first step toward the development of biopolymer-based colorimetric sensors that use structural color as a transduction mechanism.

■ ASSOCIATED CONTENT

Supporting Information

The Supporting Information is available free of charge on the ACS Publications website at DOI: 10.1021/acsami.6b02215.

Image of a green inverse opal, effect of antibody spacer length and hydrophobicity on antigen sensing, behavior of silk inverse opals in relevant buffer solutions, calculations of opal detection limit, and activity of HRP incorporated into the silk opals (PDF)

DOI: 10.1021/acsami.6b02215
ACS Appl. Mater. Interfaces XXXX, XXX, XXX−XXX

AUTHOR INFORMATION

Corresponding Authors

*Mailing address: 4 Colby Street, Science and Technology Center Room 229, Medford, MA 02155 USA. Phone: +16176274972. Fax: +16176273231. E-mail: fiorenzo.omenetto@tufts.edu.

*E-mail: david.kaplan@tufts.edu.

Author Contributions

⊥K.A.B. and M.A.B. contributed equally to this study.

Notes

The authors declare no competing financial interest.

ACKNOWLEDGMENTS

The authors wish to thank the Air Force Office of Scientific Research (FA9550-14-1-0015), as well as the National Institutes of Health for funding support in the form of the Tissue Engineering Resource Center (NIH P41 EB002520) and a Ruth Kirschstein Postdoctoral Fellowship awarded to K.A.B. (F32-DK093194). M.A.B. would like to acknowledge support from the Department of Defense, Air Force Office of Scientific Research in the form of a National Defense Science and Engineering Graduate (NDSEG) Fellowship, 32 CFR 168a.

REFERENCES

(1) Luong, J. H. T.; Male, K. B.; Glennon, J. D. Biosensor Technology: Technology Push Versus Market Pull. *Biotechnol. Adv.* **2008**, *26*, 492−500.

(2) Healy, D. A.; Hayes, C. J.; Leonard, P.; McKenna, L.; O'Kennedy, R. Biosensor Developments: Application to Prostate-Specific Antigen Detection. *Trends Biotechnol.* **2007**, *25*, 125−131.

(3) Conroy, P. J.; Hearty, S.; Leonard, P.; O'Kennedy, R. J. Antibody Production, Design and use for Biosensor-Based Applications. *Semin. Cell Dev. Biol.* **2009**, *20*, 10−26.

(4) Hock, B. Antibodies for Immunosensors. A Review. *Anal. Chim. Acta* **1997**, *347*, 177−186.

(5) Shukla, A. A.; Thömmes, J. Recent Advances in Large-Scale Production of Monoclonal Antibodies and Related Proteins. *Trends Biotechnol.* **2010**, *28*, 253−261.

(6) Shukla, A. A.; Hubbard, B.; Tressel, T.; Guhan, S.; Low, D. Downstream Processing of Monoclonal Antibodies-Application of Platform Approaches. *J. Chromatogr. B: Anal. Technol. Biomed. Life Sci.* **2007**, *848*, 28−39.

(7) Justino, C. I. L.; Freitas, A. C.; Pereira, R.; Duarte, A. C.; Rocha Santos, T. A. P. Recent Developments in Recognition Elements for Chemical Sensors and Biosensors. *TrAC, Trends Anal. Chem.* **2015**, *68*, 2−17.

(8) Wang, X.; Lu, X.; Chen, J. Development of Biosensor Technologies for Analysis of Environmental Contaminants. *Trends Environ. Anal. Chem.* **2014**, *2*, 25−32.

(9) Arugula, M. A.; Simonian, A. Novel Trends in Affinity Biosensors: Current Challenges and Perspectives. *Meas. Sci. Technol.* **2014**, *25*, 032001.

(10) Shen, Z.; Huang, M.; Xiao, C.; Zhang, Y.; Zeng, X.; Wang, P. G. Nonlabeled Quartz Crystal Microbalance Biosensor for Bacterial Detection Using Carbohydrate and Lectin Recognitions. *Anal. Chem.* **2007**, *79*, 2312−2319.

(11) Hao, R.; Wang, D.; Zhang, X.; Zuo, G.; Wei, H.; Yang, R.; Zhang, Z.; Cheng, Z.; Guo, Y.; Cui, Z.; Zhou, Y. Rapid Detection of *Bacillus Anthracis* Using Monoclonal Antibody Functionalized QCM Sensor. *Biosens. Bioelectron.* **2009**, *24*, 1330−1335.

(12) Cheng, C. I.; Chang, Y.-P.; Chu, Y.-H. Biomolecular Interactions and Tools for Their Recognition: Focus on the Quartz Crystal Microbalance and its Diverse Surface Chemistries and Applications. *Chem. Soc. Rev.* **2012**, *41*, 1947−1971.

(13) Homola, J. Surface Plasmon Resonance Sensors for Detection of Chemical and Biological Species. *Chem. Rev.* **2008**, *108*, 462−493.

(14) Karlsson, R.; Michaelsson, A.; Mattsson, L. Kinetic Analysis of Monoclonal Antibody-Antigen Interactions with a New Biosensor Based Analytical System. *J. Immunol. Methods* **1991**, *145*, 229−240.

(15) Mayer, K. M.; Lee, S.; Liao, H.; Rostro, B. C.; Fuentes, A.; Scully, P. T.; Nehl, C. L.; Hafner, J. H. A Label-Free Immunoassay Based Upon Localized Surface Plasmon Resonance of Gold Nanorods. *ACS Nano* **2008**, *2*, 687−692.

(16) Piliarik, M.; Bocková, M.; Homola, J. Surface Plasmon Resonance Biosensor for Parallelized Detection of Protein Biomarkers in Diluted Blood Plasma. *Biosens. Bioelectron.* **2010**, *26*, 1656−1661.

(17) Byrne, B.; Stack, E.; Gilmartin, N.; O'Kennedy, R. Antibody-Based Sensors: Principles, Problems and Potential for Detection of Pathogens and Associated Toxins. *Sensors* **2009**, *9*, 4407−4445.

(18) Bini, E.; Knight, D. P.; Kaplan, D. L. Mapping Domain Structures in Silks from Insects and Spiders Related to Protein Assembly. *J. Mol. Biol.* **2004**, *335*, 27−40.

(19) Vepari, C.; Kaplan, D. L. Silk as a Biomaterial. *Prog. Polym. Sci.* **2007**, *32*, 991−1007.

(20) Zhou, C. Z.; Confalonieri, F.; Jacquet, M.; Perasso, R.; Li, Z. G.; Janin, J. Silk Fibroin: Structural Implications of a Remarkable Amino Acid Sequence. *Proteins: Struct., Funct., Genet.* **2001**, *44*, 119−122.

(21) Murphy, A. R.; Kaplan, D. L. Biomedical Applications of Chemically-Modified Silk Fibroin. *J. Mater. Chem.* **2009**, *19*, 6443−6450.

(22) Hu, X.; Kaplan, D. L.; Cebe, P. Determining Beta-Sheet Crystallinity in Fibrous Proteins by Thermal Analysis and Infrared Spectroscopy. *Macromolecules* **2006**, *39*, 6161−6170.

(23) Hu, X.; Tang-Schomer, M. D.; Huang, W.; Xia, X. X.; Weiss, A. S.; Kaplan, D. L. Charge-Tunable Autoclaved Silk-Tropoelastin Protein Alloys that Control Neuron Cell Responses. *Adv. Funct. Mater.* **2013**, *23*, 3875−3884.

(24) Hu, X.; Shmelev, K.; Sun, L.; Gil, E. S.; Park, S. H.; Cebe, P.; Kaplan, D. L. Regulation of Silk Material Structure by Temperature-Controlled Water Vapor Annealing. *Biomacromolecules* **2011**, *12*, 1686−1696.

(25) Gil, E. S.; Park, S. H.; Hu, X.; Cebe, P.; Kaplan, D. L. Impact of Sterilization on the Enzymatic Degradation and Mechanical Properties of Silk Biomaterials. *Macromol. Biosci.* **2014**, *14*, 257−269.

(26) Rnjak-Kovacina, J.; Desrochers, T. M.; Burke, K. A.; Kaplan, D. L. The Effect of Sterilization on Silk Fibroin Biomaterial Properties. *Macromol. Biosci.* **2015**, *15*, 861−874.

(27) De Moraes, M. A.; Weska, R. F.; Beppu, M. M. Effects of Sterilization Methods on the Physical, Chemical, and Biological Properties of Silk Fibroin Membranes. *J. Biomed. Mater. Res., Part B* **2014**, *102*, 869−876.

(28) Hofmann, S.; Stok, K. S.; Kohler, T.; Meinel, A. J.; Müller, R. Effect of Sterilization on Structural and Material Properties of 3-D Silk Fibroin Scaffolds. *Acta Biomater.* **2014**, *10*, 308−317.

(29) Kim, S.; Mitropoulos, A. N.; Spitzberg, J. D.; Tao, H.; Kaplan, D. L.; Omenetto, F. G. Silk Inverse Opals. *Nat. Photonics* **2012**, *6*, 818−823.

(30) Swinerd, V. M.; Collins, A. M.; Skaer, N. J. V.; Gheysens, T.; Mann, S. Silk Inverse Opals from Template-Directed β-sheet Transformation of Regenerated Silk Fibroin. *Soft Matter* **2007**, *3*, 1377−1380.

(31) Diao, Y. Y.; Liu, X. Y.; Toh, G. W.; Shi, L.; Zi, J. Multiple Structural Coloring of Silk-Fibroin Photonic Crystals and Humidity-Responsive Color Sensing. *Adv. Funct. Mater.* **2013**, *23*, 5373−5380.

(32) Kim, S.; Mitropoulos, A. N.; Spitzberg, J. D.; Kaplan, D. L.; Omenetto, F. G. Silk Protein Based Hybrid Photonic-Plasmonic Crystal. *Opt. Express* **2013**, *21*, 8897−8903.

(33) Lee, S. Y.; Amsden, J. J.; Boriskina, S. V.; Gopinath, A.; Mitropolous, A.; Kaplan, D. L.; Omenetto, F. G.; Dal Negro, L. Spatial and spectral Detection of Protein Monolayers with Deterministic Aperiodic Arrays of Metal Nanoparticles. *Proc. Natl. Acad. Sci. U. S. A.* **2010**, *107*, 12086−12090.

DOI: 10.1021/acsami.6b02215
ACS Appl. Mater. Interfaces XXXX, XXX, XXX−XXX

(34) Boriskina, S. V.; Lee, S. Y. K.; Amsden, J. J.; Omenetto, F. G.; Dal Negro, L. Formation of Colorimetric Fingerprints on Nano-Patterned Deterministic Aperiodic Surfaces. *Opt. Express* **2010**, *18*, 14568−14576.
(35) Amsden, J. J.; Perry, H.; Boriskina, S. V.; Gopinath, A.; Kaplan, D. L.; Dal Negro, L.; Omenetto, F. G. Spectral Analysis of Induced Color Change on Periodically Nanopatterned Silk Films. *Opt. Express* **2009**, *17*, 21271−21279.
(36) Cronin-Golomb, M.; Murphy, A. R.; Mondia, J. P.; Kaplan, D. L.; Omenetto, F. G. Optically Induced Birefringence and Holography in Silk. *J. Polym. Sci., Part B: Polym. Phys.* **2012**, *50*, 257−262.
(37) Pal, R. K.; Kurland, N. E.; Wang, C.; Kundu, S. C.; Yadavalli, V. K. Biopatterning of Silk Proteins for Soft Micro-Optics. *ACS Appl. Mater. Interfaces* **2015**, *7*, 8809−8816.
(38) Lawrence, B. D.; Cronin-Golomb, M.; Georgakoudi, I.; Kaplan, D. L.; Omenetto, F. G. Bioactive Silk Protein Biomaterial Systems for Optical Devices. *Biomacromolecules* **2008**, *9*, 1214−1220.
(39) Kurland, N. E.; Dey, T.; Kundu, S. C.; Yadavalli, V. K. Precise Patterning of Silk Microstructures Using Photolithography. *Adv. Mater.* **2013**, *25*, 6207−6212.
(40) Tao, H.; Kainerstorfer, J. M.; Siebert, S. M.; Pritchard, E. M.; Sassaroli, A.; Panilaitis, B. J. B.; Brenckle, M. A.; Amsden, J. J.; Levitt, J.; Fantini, S.; Kaplan, D. L.; Omenetto, F. G. Implantable, Multifunctional, Bioresorbable Optics. *Proc. Natl. Acad. Sci. U. S. A.* **2012**, *109*, 19584−19589.
(41) Mondia, J. P.; Amsden, J. J.; Lin, D.; Negro, L. D.; Kaplan, D. L.; Omenetto, F. G. Rapid Nanoimprinting of Doped Silk Films for Enhanced Fluorescent Emission. *Adv. Mater.* **2010**, *22*, 4596−4599.
(42) Tao, H.; Brenckle, M. A.; Yang, M.; Zhang, J.; Liu, M.; Siebert, S. M.; Averitt, R. D.; Mannoor, M. S.; McAlpine, M. C.; Rogers, J. A.; Kaplan, D. L.; Omenetto, F. G. Silk-Based Conformal, Adhesive, Edible Food Sensors. *Adv. Mater.* **2012**, *24*, 1067−1072.
(43) Rockwood, D. N.; Preda, R. C.; Yucel, T.; Wang, X.; Lovett, M. L.; Kaplan, D. L. Materials Fabrication from *Bombyx mori* Silk Fibroin. *Nat. Protoc.* **2011**, *6*, 1612−1631.
(44) González, M.; Argaraña, C. E.; Fidelio, G. D. Extremely High Thermal Stability of Streptavidin and Avidin upon Biotin Binding. *Biomol. Eng.* **1999**, *16*, 67−72.
(45) Wilchek, M.; Bayer, E. A. The Avidin-Biotin Complex in Bioanalytical Applications. *Anal. Biochem.* **1988**, *171*, 1−32.
(46) Burke, K. A.; Roberts, D. C.; Kaplan, D. L. Silk Fibroin Aqueous-Based Adhesives Inspired by Mussel Adhesive Proteins. *Biomacromolecules* **2016**, *17*, 237−245.
(47) Serban, M. A.; Kaplan, D. L. pH-Sensitive Ionomeric Particles Obtained via Chemical Conjugation of Silk with Poly(amino acid)s. *Biomacromolecules* **2010**, *11*, 3406−3412.
(48) Wang, X.; Kaplan, D. L. Functionalization of Silk Fibroin with NeutrAvidin and Biotin. *Macromol. Biosci.* **2011**, *11*, 100−110.
(49) Lu, Q.; Wang, X.; Zhu, H.; Kaplan, D. L. Surface Immobilization of Antibody on Silk Fibroin Through Conformational Transition. *Acta Biomater.* **2011**, *7*, 2782−2786.
(50) Miller, P. R.; Skoog, S. A.; Edwards, T. L.; Lopez, D. M.; Wheeler, D. R.; Arango, D. C.; Xiao, X.; Brozik, S. M.; Wang, J.; Polsky, R.; Narayan, R. J. Multiplexed Microneedle-Based Biosensor Array for Characterization of Metabolic Acidosis. *Talanta* **2012**, *88*, 739−742.
(51) Kuralay, F.; Campuzano, S.; Haake, D. A.; Wang, J. Highly Sensitive Disposable Nucleic Acid Biosensors for Direct Bioelectronic Detection in Raw Biological Samples. *Talanta* **2011**, *85*, 1330−1337.
(52) Wang, Y.; Zhang, Z.; Jain, V.; Yi, J.; Mueller, S.; Sokolov, J.; Liu, Z.; Levon, K.; Rigas, B.; Rafailovich, M. H. Potentiometric Sensors Based on Surface Molecular Imprinting: Detection of Cancer Biomarkers and Viruses. *Sens. Actuators, B* **2010**, *146*, 381−387.
(53) Pohanka, M.; Pavlis, O.; Skladal, P. Rapid Characterization of Monoclonal Antibodies Using the Piezoelectric Immunosensor. *Sensors* **2007**, *7*, 341−353.

DOI: 10.1021/acsami.6b02215
ACS Appl. Mater. Interfaces XXXX, XXX, XXX−XXX